Normal and Anomalous Diffusion in Soft Lorentz Gases: Supplemental Material

Rainer Klages,[1,2,3,*] Sol Selene Gil Gallegos,[1] Janne Solanpää,[4] Mika Sarvilahti,[4] and Esa Räsänen[4]

[1] *Queen Mary University of London, School of Mathematical Sciences, Mile End Road, London E1 4NS, UK*
[2] *Institut für Theoretische Physik, Technische Universität Berlin, Hardenbergstraße 36, 10623 Berlin, Germany*
[3] *Institute for Theoretical Physics, University of Cologne, Zülpicher Straße 77, 50937 Cologne, Germany*
[4] *Computational Physics Laboratory, Tampere University, P.O. Box 692, FI-33014 Tampere, Finland*

(Dated: January 28, 2019)

I. TECHNICAL DETAILS OF THE NUMERICAL SIMULATIONS

The numerical simulations were carried out with the *bill2d* software package [1] for classical dynamics. The time-propagation was performed using the 4th order algorithm of Yoshida [2]. We employed a parallelogram, non-primitive unit cell containing four Fermi potentials. The full potential was represented as a sum over all Fermi potentials Eq.(1) in the unit cell and in its next and next-nearest neighboring unit cells. For the figures in the main part we performed high precision computations with an ensemble size of $\geq 10^5$ trajectories that guaranteed a vanishingly small standard error of the mean in Eq.(2). The initial conditions were sampled uniformly in the coordinate space of the unit cell, the initial speeds of the particles were fixed to satisfy the total energy condition ($E = 1/2$), and the initial launch angles were randomized. A numerical estimate for the diffusion coefficient D Eq.(2) was obtained with a linear fit to $\langle(\mathbf{r}(t) - \mathbf{r}(0))^2\rangle$ as a function of time, where we skipped the initial transient region and instead made a fit at $t = 1000 \ldots 5000$. The two figures shown later in this Supplement were generated with less precision than in the main part. In both cases we iterated up to time $t = 5000$ with a time step of 10^{-3}. For Fig. 1 we chose an ensemble size of 10000 particles, for Fig. 2 we had 100000 particles.

II. RANDOM WALK APPROXIMATIONS FOR DIFFUSION

In order to understand the coarse scale parameter dependence of the diffusion coefficient $D(w)$ depicted in Fig. 2 we employ a Boltzmann-type random walk approximation, which was put forward in Ref. [3], see Sec. 4 therein. As briefly described in the main text, this approximation is based on the assumption that diffusion is governed by 'flights' of length $\ell_c = \ell_c(w)$ over corresponding flight time intervals $\tau_c = \tau_c(w)$ after which a particle experiences a 'collision'. However, in contrast to the standard Lorentz gas with hard walls studied in [3] our potential is soft. Hence, here we define a collision as an event where a particle hits the contour line of a scatterer at $E = 1/2$ in the triangular unit cell A displayed in Fig. 1 of the main text. By assuming that all collisions are uncorrelated the diffusion coefficient can be approximated as

$$D_B(w) = \frac{\ell_c^2}{4\tau_c} \quad . \tag{1}$$

In the hard Lorentz gas τ_c can be calculated using a phase space argument analogous to the one that was put forward in Ref. [4] to compute the mean escape time τ_e of a particle out of a unit cell. The latter can be expressed in terms of the probability to leave a trap within the time τ_e. This quantity is in turn given by the portion of the phase space from which a particle can escape from a trap during time τ_e divided by the total phase space volume of a trap; for details we refer to [4]. The only difference for computing τ_c is that here one replaces the flux across the exits of a trap by the flux to the walls bounding the trap. Working this out for our soft Lorentz gas we get

$$\tau_c^{-1} = \frac{v}{A} \quad . \tag{2}$$

Here $A = A(w)$ is the accessible area for the particle in position space, and $v = |\mathbf{v}(w)|$ defines the average constant speed with which a particle travels between collisions. We now have everything at hand to boil down Eq.(1) to

*Electronic address: r.klages@qmul.ac.uk

something computable: First, using $l_c = v\tau_c$ in Eq.(1) we trivially obtain

$$D_B(w) = \frac{v^2\tau_c}{4} \quad . \tag{3}$$

Substituting τ_c by Eq.(2) yields

$$D_B(w) = \frac{A}{4}v \quad . \tag{4}$$

A is easily computed by geometric arguments leading to our central formula

$$D_B(w) = \frac{\sqrt{3}L^2/4 - \pi r_0^2/2}{4}v \quad , \tag{5}$$

where L is the lattice spacing. It remains to calculate v. For this recall that a particle moves in the plane under the influence of overlapping Fermi potentials, see Eq.(1) in the main text. This means the kinetic energy varies depending on the position of the particle, consequently the speed fluctuates as well. However, as explained above, for Eq.(5) we assume that a particle travels with an on average constant speed v. We define this speed in two ways by using the following approximations:

1. We calculate *analytically* an *approximate average speed* $v_{\text{ave}} = v_{\text{ave}}(w)$ at the moment when a particle leaves A. For this we consider the contributions of the potential from two adjacent lattice points in the plane only. Without loss of generality we may choose $(0, 0)$ and $(L, 0)$ located at the centres of two nearby potentials $V_1(x) := V_1(x, 0)$ and $V_2(x) := V_2(L, 0)$ with $L = 2r_0 + w$. Note that with the latter equation for the lattice spacing we approximate the true gap size in the case of overlapping Fermi potentials by a gap size w derived from using a single non-overlapping Fermi potential; see Ref. [5] for details. By considering the contributions from these two potentials along the x-axis the joint potential $V_j(x)$ reads

$$V_j(x) = V_1(x) + V_2(x) = \frac{1}{1 + \exp((|x| - r_0)/\sigma)} + \frac{1}{1 + \exp(|x - L| - r_0)/\sigma)} \quad . \tag{6}$$

   We now define an average potential V_{ave} over the approximate exit of a trap according to

$$V_{\text{ave}}(w) = \frac{1}{w}\int_{r_0}^{r_0+w} V_j(x)dx \quad . \tag{7}$$

   Exploiting symmetry this integral can be calculated to

$$V_{\text{ave}}(w) = 2 + \frac{2\sigma}{w}\ln\left(\frac{2}{1 + \exp(w/\sigma)}\right) \quad . \tag{8}$$

   Conservation of energy yields $v = \sqrt{2(E - V_j(x))}$. Combining this with Eq. (8), an average exit speed can be expressed as

$$v_{\text{ave}}(w) = \sqrt{2(E - V_{\text{ave}}(w))} \quad . \tag{9}$$

2. A second definition is based on calculating *numerically* the *correct average speed* $v_{\text{num}} = v_{\text{num}}(w)$ while a particle is leaving a trap. Using symmetry we have to compute the integral

$$v_{\text{num}} = \frac{2}{w}\int_{r_\epsilon}^{r_\epsilon + w/2} \sqrt{2\left(E - V_{\text{tot}}(x)\right)}\,\mathrm{d}x, \tag{10}$$

   where $V_{\text{tot}}(x) := V_{\text{tot}}(x, 0)$ is the sum over the range of potentials as defined in Sec. I above. Note that this requires us to compute r_ϵ defined by $V_{\text{tot}}(r_\epsilon) = 1/2$ due to the overlapping potentials. This integral is not solvable analytically, hence we compute it numerically.

Using these two approximations for the speed v in Eq.(5) yields our two approximations D_B and $D_{B,num}$ plotted in Fig. 2 of the main text.

III. TRANSITION BETWEEN THE SOFT AND THE HARD LORENTZ GAS

In this section we discuss first qualitatively and then quantitatively the changes of the diffusive dynamics in the hard disk Lorentz gas when softening the scatterers. In Subsec. A we outline generic dynamical systems properties of both models by discussing their similarities and differences. Subsection B presents computer simulation results for the diffusion coefficient as a function of the smoothness parameter σ exploring this transition in more depth when σ is getting smaller.

A. The hard and the soft Lorentz gas: Similarities and differences in their diffusive dynamics

Diffusion in the conventional Lorentz gas consisting of a point particle scattering with hard disks has been studied in a large number of works; see [6–10] for reviews. Pioneering mathematical research by Bunimovich and Sinai showed rigorously that the Lorentz gas is a K-system, which implies that it is mixing and ergodic [11, 12]. It is furthermore a hyperbolic chaotic dynamical system [13]. For the two-dimensional periodic Lorentz gas with scatterers situated on a triangular lattice these strong chaos properties imply that diffusion is normal in the parameter regime of the gap size w of $0 < w < w_\infty$, in the sense that the mean square displacement (MSD) grows linearly with time in the long-time limit, as was proven in Ref. [11]. In this regime the diffusion coefficient as a function of w was explored in Refs. [3, 4, 14–16]. The result from simulations of $D(w)$ is shown in the inset of Fig. 2 in the main text. While in this plot D looks like a rather smooth function of w it was shown in Ref. [3] that there are irregularities in the form of slight wiggles on very fine scales. The order of magnitude of these irregularities is by far smaller than in the soft model, cp. Fig. 2 in the main text for the soft Lorentz gas with Fig. 1(b) in [3]. So far it is only known that these irregularities exist in the conventional Lorentz gas, but they could not be explained, e.g., in terms of periodic orbits. There are attempts in the literature, however, to compute $D(w)$ for the hard periodic Lorentz gas in terms of *unstable* periodic orbits [17–19].

Note that $w_\infty = 4\sqrt{3} - 3 \simeq 0.3094$ defines the onset of an *infinite horizon* in the periodic Lorentz gas, where a particle can for the first time move ballistically along infinite channels across the entire lattice without colliding with any scatterer. Accordingly, for $w_\infty > w$ diffusion becomes anomalous, and D as defined by Eq. (2) in the main text does not exist anymore. This is reflected in our chart of periodic orbits in Fig. 4 (main part) as the big red tongue of quasi-ballistic periodic orbits emerging from $w \simeq 0.31$ for small σ. More precisely, infinite horizon Lorentz gases exhibit a special type of superdiffusion, where the MSD grows like $t \ln t$. This is due to a family of strictly ballistic periodic orbits which, however, occupy only zero volume in the whole phase space of the system [20–25].

In marked contrast to this hard Lorentz gas scenario of purely chaotic deterministic diffusion with a well-defined diffusion coefficient for $w < w_\infty$, and superdiffusion for $w > w_\infty$ due to an infinite horizon, in our main text we have shown that softening the hard disks by using overlapping Fermi potentials changes the diffusive dynamics profoundly: Even a minimal softening of the potential yields a mixed phase space [26] composed of chaotic regions interrupted by small 'islands' of periodic orbits, cf. Fig. 3 (main part). Note that in contrast to the hard Lorentz gas these islands occupy non-zero volume and are *stable* in phase space. This implies a completely different type of non-hyperbolic dynamics compared to the well-behaved hard Lorentz gas which, in turn, is reflected in profound changes of the corresponding diffusive properties. In turn, it is well-known that islands of periodicity in phase space corresponding to 'propagating' periodic orbits, also called accelerator modes, lead to superdiffusion, even if they are very tiny, while parameter regions without any islands correspond to normal diffusion [27–32].

At first view this phenomenon may look similar to the infinite horizon case in the hard periodic Lorentz gas. But in the soft model the orbits generating superdiffusion are not strictly 'ballistic' in the sense of being collision-free, as is demonstrated by Fig. 3 (main text). Rather particles collide with the scatterers in intricate ways while they move on average in one direction. Hence there are no infinite horizon channels in our soft system, as there is always a force acting on a particle, therefore we call these trajectories *quasi-ballistic*. Secondly, in contrast to the hard Lorentz gas the phase space of a quasi-ballistic island of periodicity is non-zero, due to the velocity now representing an additional degree of freedom. This implies a generically different type of superdiffusion compared to the hard Lorentz gas infinite horizon case with a MSD that grows like t^α , $\alpha > 1$ [20–25].

To our knowledge so far there are no works that study the transition from Hamiltonian particle billiards consisting of hard walls, like Lorentz gases, to systems consisting of soft periodic potentials, like our model, as far as diffusion is concerned. The only research we are aware of is a series of articles by Turaev and Rom-Kedar, who investigate in mathematical depth the changes of the dynamics by softening the hard walls of billiards, however, without exploring the impact on diffusive properties [33, 34]. There is a claim in these references that under softening hard walls islands of periodicity become typical in parameter space, but this has not been observed in parameter space as shown in our Fig. 4. We also remark that the theory by Turaev and Rom-Kedar predicts that for small σ the tongues of periodic orbits depicted in Fig. 4 should grow linearly in parameter space, see Theorem 1 in Ref. [34]. But to verify this

numerically is at present out of reach, as it is extremely difficult to find small islands of periodicity especially for σ close to zero.

B. The diffusion coefficient as a function of the smoothness parameter

We now explore the transition between the hard and the soft Lorentz gas regarding their diffusive properties in more depth. In the main text we have focused on the diffusion coefficient as a function of the gap size w between two adjacent scatterers for fixed smoothness parameter σ, cf. Fig. 2. Here we first present results for the diffusion coefficient D at fixed w under variation of σ. This supplements our previous analysis related to the chart of periodic orbits shown in Fig. 4, main part: While so far we have explored the parameter space displayed therein along horizontal cuts through this plane, in the following we elucidate what happens along vertical cuts. This sheds light on the transition of diffusive properties between the soft and the hard scatterer case when σ is close to zero.

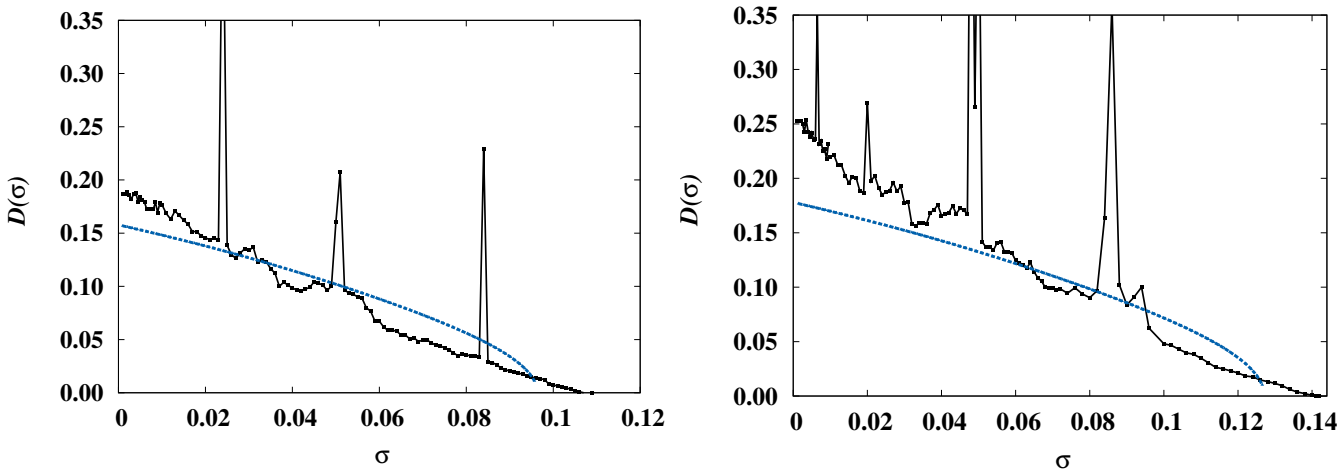

FIG. 1: Diffusion coefficient D as a function of the smoothness parameter σ when the gap size is fixed to $w = 0.235$ (left) and $w = 0.31$ (right). The black lines with symbols represent results from computer simulations. The peaks therein correspond to parameter regions where the diffusion coefficient has not converged to a final value due to the existence of quasi-ballistic periodic orbits. The (blue) dashed lines give the simple random walk approximation $D_{\mathrm{MZ}}(\sigma)$ Eq. (11).

Figure 1 (a) and (b) depict results for $D(\sigma)$ at two fixed values of w. These two figures correspond to vertical cuts in Fig. 4 (main text) from top to bottom by showing what happens when σ approaches zero. We see that in both cases $D(\sigma)$ is an increasing function when decreasing σ. However, as in case of $D(w)$ for fixed σ in Fig. 2 (main text), we observe again irregularities on finer scales. They are supplemented by peaks representing parameter regions where D has not converged to a final value, as it does not exist due to the existence of quasi-ballistic periodic orbits. These peaks match to respective quasi-ballistic tongues in Fig. 4 (main text). Note, however, that in the left figure the lowest tongue around $\sigma \simeq 0.01$ has been missed. This may be due to the chosen spacing between two adjacent data points $D(\sigma)$, or that our initial ensemble did not catch a respective tiny island of stability. The values of $D(0)$ correspond to the respective results for the hard Lorentz gas shown in the inset of Fig. 2 (main text).

The blue dashed lines are analytical results representing a simple random walk approximation put forward by Machta and Zwanzig [4], suitably adapted to the soft Lorentz gas: The assumption is that particles hop from trap to trap on a triangular lattice, cf. Fig. 1 (main text) for the trapping region A with an escape time τ_e from each trap, where the centres of the traps are a distance $\ell = L/\sqrt{3}$ apart. By assuming no memory between two jumps, similarly to Eq. (1) above yielding our Boltzmann approximation the diffusion coefficient can be approximated to

$$D_{\mathrm{MZ}}(\sigma) = \frac{\ell^2}{4\tau_e} \quad . \tag{11}$$

Again in analogy to the Boltzmann approximation τ_e is now given again by a phase space argument,

$$\tau_e^{-1} = \frac{3wv}{\pi A} \quad , \tag{12}$$

where, as explained in Sec. I in the Supplement, the only difference to the collision time τ_c in Eq. (2) is that for calculating the escape time τ_e we consider the portion of phase space where a particle leaves a trap. Combining

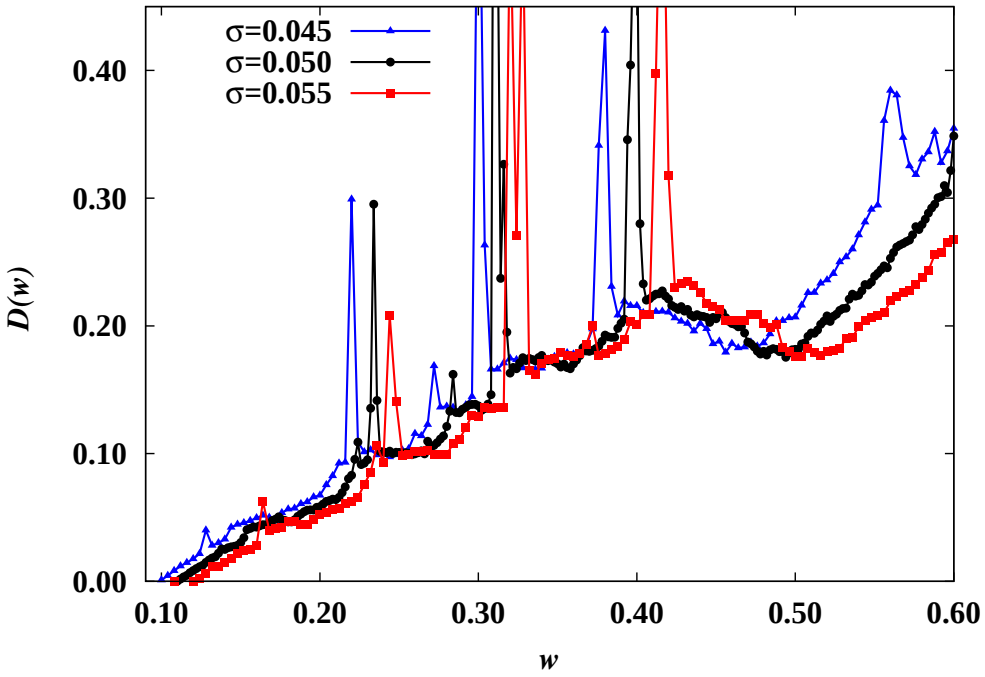

FIG. 2: Diffusion coefficient $D(w)$ obtained from simulations for three different values of the smoothness parameter σ as given in the figure.

Eq. (12) with Eq. (11) by plugging in the value for A as before yields

$$D_{\mathrm{MZ}}(\sigma) = \frac{L^2 w}{\pi(\sqrt{3}L^2 - 2\pi)} v \quad . \tag{13}$$

In Fig. 1 above we have used this formula by replacing v with the average velocity calculated in Eqs. (8),(9) above, $v = v_{ave}$, which yields the dashed blue lines. We see that this analytical random walk approximation matches qualitatively to the numerical results by particularly explaining the increase of the (normal) diffusion coefficient when the system approaches the hard Lorentz gas limit for small σ. Note that the quantitative mismatch between the data and the approximation is increasing from $\sigma \to 0$, as is analysed in detail in [3, 14]. What we can learn from Fig. 1 and its analysis is that the transition between diffusion in the soft and the hard Lorentz gas for σ close to zero looks smooth on a coarse grained level as far as the diffusion coefficient is concerned when it exists, as is confirmed by our random walk approximation. However, whenever quasi-ballistic islands of periodicity occur, they interrupt this scenario. Increasing the numerical precision will reveal more and more superdiffusive parameter regions, probably even an infinite set of them, thus severely disrupting any smooth transition scenario. This result is fully in line with our chart of periodic orbits Fig. 4 (main text) by illustrating it in detail for $D(\sigma)$.

We finish our discussion of the impact of the smoothness parameter on diffusion in the soft Lorentz gas by presenting numerical results for $D(w)$ at three different values of σ, see Fig. 2. The shift of the different peaks, where diffusion is anomalous, to the left when σ is getting smaller is again fully in line with our chart of periodic orbits Fig. 4 (main text). We see that the whole curve where the normal diffusion coefficient exists is slightly deforming under variation of σ: Except in a tiny parameter region of $0.4 < w < 0.5$ overall it is increasing when σ is getting smaller, i.e., when the soft system is approaching the hard Lorentz gas limit. Within the parameter region of $0 < w < 0.31$ eventually it will converge to the known diffusion coefficient of the hard Lorentz shown in the inset of Fig. 2 (main text) while the whole parameter region for $w > 0.31$ will gradually become superdiffusive.

[1] J. Solanpää, P. Luukko, and E. Räsänen, Comp. Phys. Commun. **199**, 133 (2016).
[2] H. Yoshida, Phys. Lett. A **150**, 262 (1990).
[3] R. Klages and C. Dellago, J. Stat. Phys. **101**, 145 (2000).
[4] J. Machta and R. Zwanzig, Phys. Rev. Lett. **50**, 1959 (1983).
[5] S. S. Gil Gallegos, Ph.D. thesis, Queen Mary University of London (2018).
[6] P. Gaspard, *Chaos, scattering, and statistical mechanics* (Cambridge University Press, Cambridge, 1998).
[7] J. R. Dorfman, *An introduction to chaos in nonequilibrium statistical mechanics* (Cambridge University Press, Cambridge, 1999).
[8] R. Klages, *Microscopic chaos, fractals and transport in nonequilibrium statistical mechanics*, (World Scientific, Singapore, 2007).
[9] D. Szasz, ed., *Hard-ball systems and the Lorentz gas*, vol. 101 of *Encyclopedia of mathematical sciences* (Springer, Berlin, 2000).
[10] C. P. Dettmann, Comm. Theor. Phys. **62**, 521 (2014).
[11] L. A. Bunimovich and Ya. G. Sinai, Commun. Math. Phys. **78**, 247 (1980).
[12] L. A. Bunimovich and Ya. G. Sinai, Commun. Math. Phys. **78**, 479 (1981).
[13] Ya. G. Sinai, Russ. Math. Surv. **25**, 137 (1970).
[14] R. Klages and N. Korabel, J. Phys. A: Math. Gen. **35**, 4823 (2002).
[15] T. Gilbert and D. P. Sanders, Phys. Rev. E **80**, 041121/1 (2009).
[16] C. Angstmann and G. Morriss, Phys. Lett. A **376**, 1819 (2012).
[17] P. Cvitanović, P. Gaspard, and T. Schreiber, Chaos **2**, 85 (1992).
[18] P. Cvitanović, J.-P. Eckmann, and P. Gaspard, Chaos, Solitons and Fractals **6**, 113 (1995).
[19] P. Cvitanović, R. Artuso, R. Mainieri, G. Tanner, and G. Vattay, *Chaos: Classical and quantum* (Niels Bohr Institute, Copenhagen, 2007).
[20] A. Zacherl, T. Geisel, J. Nierwetberg, and G. Radons, Phys. Lett. **114A**, 317 (1986).
[21] R. M. Feliczaki, E. Vicentini, and P. P. González-Borrero, Phys. Rev. E **96**, 052117 (2017).
[22] C. P. Dettmann, J. Stat. Phys. **146**, 181 (2012).
[23] G. Cristadoro, T. Gilbert, M. Lenci, and D. P. Sanders, Phys. Rev. E **90**, 050102 (2014).
[24] G. Cristadoro, T. Gilbert, M. Lenci, and D. P. Sanders, Phys. Rev. E **90**, 022106 (2014).
[25] L. Zarfaty, A. Peletskyi, I. Fouxon, S. Denisov, and E. Barkai, Phys. Rev. E **98**, 010101 (2018).
[26] A. Lichtenberg and M. Lieberman, *Regular and chaotic dynamics*, (Springer, New York, 1992), 2nd ed.
[27] T. Geisel, A. Zacherl, and G. Radons, Phys. Rev. Lett. **59**, 2503 (1987).
[28] T. Geisel, A. Zacherl, and G. Radons, Z. Phys. B **71**, 117 (1988).
[29] G. Zaslavsky, Phys. Rep. **371**, 461 (2002).
[30] R. Klages, G. Radons, and I. M. Sokolov, eds., *Anomalous transport: Foundations and Applications* (Wiley-VCH, Berlin, 2008).
[31] T. Manos and M. Robnik, Phys. Rev. E **89**, 022905 (2014).
[32] M. Harsoula and G. Contopoulos, Phys. Rev. E **97**, 022215 (2018).
[33] D. Turaev and V. Rom-Kedar, Nonlinearity **11**, 575 (1998).
[34] V. Rom-Kedar and D. Turaev, Physica D **130**, 187 (1999).